A symptomatic Fabry disease mouse model generated by inducing globotriaosylceramide synthesis

Atsumi TAGUCHI*, Hiroki MARUYAMA†[1], Masaaki NAMETA‡, Tadashi YAMAMOTO‡, Junichiro MATSUDA§, Ashok B. KULKARNI∥, Hidekatsu YOSHIOKA* and Satoshi ISHII*¶[1,2,3]

*Department of Matrix Medicine, Faculty of Medicine, Oita University, Yufu, Oita 879-5593, Japan, †Department of Clinical Nephroscience, Niigata University Graduate School of Medical and Dental Sciences, Niigata 951-8120, Japan, ‡Electron Microscope Core Facility, Niigata University, Niigata 951-8120, Japan, §Laboratory of Animal Models for Human Diseases, National Institute of Biomedical Innovation, Osaka 567-0085, Japan, ∥National Institute of Dental and Craniofacial Research, National Institutes of Health, Bethesda, MD 20892, U.S.A., and ¶Biochemical Laboratory, GlycoPharma Corporation, Oita 870-0822, Japan

Fabry disease is a lysosomal storage disorder in which neutral glycosphingolipids, predominantly Gb3 (globotriaosylceramide), accumulate due to deficient α-Gal A (α-galactosidase A) activity. The GLAko (α-Gal A-knockout) mouse has been used as a model for Fabry disease, but it does not have any symptomatic abnormalities. In the present study, we generated a symptomatic mouse model (G3Stg/GLAko) by cross-breeding GLAko mice with transgenic mice expressing human Gb3 synthase. G3Stg/GLAko mice had high Gb3 levels in major organs, and their serum Gb3 level at 5–25 weeks of age was 6–10-fold higher than that in GLAko mice of the same age. G3Stg/GLAko mice showed progressive renal impairment, with

albuminuria at 3 weeks of age, decreased urine osmolality at 5 weeks, polyuria at 10 weeks and increased blood urea nitrogen at 15 weeks. The urine volume and urinary albumin concentration were significantly reduced in the G3Stg/GLAko mice when human recombinant α-Gal A was administered intravenously. These data suggest that Gb3 accumulation is a primary pathogenic factor in the symptomatic phenotype of G3Stg/GLAko mice, and that this mouse line is suitable for studying the pathogenesis of Fabry disease and for preclinical studies of candidate therapies.

Key words: enzyme replacement therapy, Fabry disease, globotriaosylceramide synthesis, symptomatic mouse model.

INTRODUCTION

Fabry disease is an X-linked inherited lysosomal storage disorder in which glycosphingolipids, predominantly Gb3 (globotriaosylceramide), accumulate in visceral tissues and body fluids due to deficient α-Gal A (α-galactosidase A) enzymatic activity [1]. Gb3 accumulation results in a progressive disorder characterized by cardiac disease, chronic renal insufficiency and cerebrovascular stroke [2]. Without medical treatment, patients eventually suffer from renal failure or cerebrovascular disease in their 40s or 50s [3,4]. Affected hemizygous males without detectable α-Gal A activity generally have severe clinical symptoms. Heterozygous females with intermediate α-Gal A activity are usually asymptomatic, but may develop vascular heart and kidney disease at a later age than males do [5].

The GLAko (α-Gal A-knockout) mouse has been used as a model for Fabry disease [6]. Although GLAko mice accumulate Gb3 in their organs, they have a normal lifespan and do not have a Fabry disease phenotype. Gb3 accumulates in the GLAko mouse liver and kidneys with age, but the kidney Gb3 concentration only reaches 25 % of that found in patients with Fabry disease [7]. We hypothesized that GLAko mice lack phenotypic manifestations because mice have a lower capacity than humans for synthesizing Gb3, and that increasing the organ Gb3 synthesis might provide a phenotypic model mouse for Fabry disease.

Currently, Fabry disease can be treated with ERT (enzyme replacement therapy) using infusions of recombinant human

α-Gal A (agalsidase-α or agalsidase-β) [8,9]. However, the treatment is expensive (approximately \$200 000/patient per year [10]) and it has side effects related to the immunogenicity of the recombinant enzyme [11]. Other therapies proposed for Fabry disease include bone marrow transplantation [7], gene therapy [12], SRT (substrate reduction therapy) [13,14] and pharmacological chaperone therapy [15,16]. Preclinical studies have examined the effect of these therapies [7,12,14] on the Gb3 levels in GLAko mice; however, there is no guarantee that reducing the Gb3 levels in GLAko mice will translate to a therapeutic effect in human Fabry disease. In a preclinical SRT study using a mouse model for Sandhoff disease, a neuropathic glycosphingolipidosis caused by a lysosomal β-hexosaminidase deficiency, the administration of SRT candidates increased mouse survival and protected against neuronal damage without reducing glycosphingolipid accumulations in the brain [17]. These findings indicate that we still do not completely understand the pathogenesis of glycosphingolipidosis, and that a symptomatic mouse model is urgently needed for effective preclinical studies of therapies for Fabry disease.

We previously generated TgG3S mice [human G3S (Gb3 synthase)-transgenic mice] with elevated Gb3 levels in major organs [18]. In the present study, we prepared a new mouse line (G3Stg/GLAko) by cross-breeding TgG3S and GLAko mice to obtain a phenotypic model for Fabry disease. In the present paper we report the characteristics of these symptomatic G3Stg/GLAko mice in comparison with asymptomatic GLAko mice.

MATERIALS AND METHODS

Animals

Transgenic (TgG3S) mice expressing human G3S, generated in our previous study [18], were maintained by breeding with wild-type C57BL/6 mice. The G3Stg/GLAko mouse line was generated by cross-breeding male TgG3S mice and homozygous female GLAko mice [6]. The G3S transgene was kept in a single allele in the TgG3S and G3Stg/GLAko mice so that the G3S expression could be consistently controlled. Studies were conducted according to the principles and procedures outlined in the Science Council of Japan's Guidelines for Proper Conduct of Animal Experiments, and were approved by the IACUC (Institutional Animal Care and Use Committee) at Oita University.

Genotyping

Mouse lines were genotyped by PCR amplification of the mouse α-Gal A (*GLA*) and human G3S (*A4GALT*) genes. DNA samples were prepared from ear-punch samples digested with protease K (TaKaRa Bio). The mouse *Gla* and knockout alleles were detected by multiplex PCR as described previously [19]. The human G3S transgene was amplified with the following primer set: 5'-TCAGTGCCACCTATGCTGTC-3' and 5'-CATATGTCCTTCCGAGTGAG-3'.

Enzyme replacement study in G3Stg/GLAko mice

Recombinant human α-Gal A (agalsidase-β; Fabrazyme®) was purchased from Genzyme. An enzyme replacement study in 5-week-old G3Stg/GLAko mice was designed to investigate the effects of a clinically relevant dose of recombinant α-Gal A (1 mg/kg) injected into the tail vein once every other week for 15 weeks.

Sample collection

To determine the daily urine volume, mice were kept individually in metabolic cages (Tecniplast Spa) for 24 h with *ad libitum* feeding. Fresh individual urine samples were collected by gently applying abdominal pressure to the mouse. Blood collected from the postcaval vein was allowed to clot for 30 min at room temperature (25 °C), and serum samples were centrifuged at 3000 *g* for 10 min to remove any remaining blood cells. Urine and serum samples were stored at -80 °C.

Determination of Gb3 content and serum lyso-Gb3 (globotriaosylsphingosine)

Neutral glycosphingolipids were extracted from each tissue and serum and the Gb3 content was determined as described previously [20]. Lyso-Gb3 extracted from serum was assayed as described previously [21].

Biochemical assay

BUN (blood urea nitrogen) levels were measured using a urease-indophenol assay kit (Wako Pure Chemicals). Urine creatinine concentrations were determined by a quantitative colorimetric assay kit using the Jaffe method (Wako Pure Chemicals).

Urine osmolality

Urine osmolality was measured with an osmometer (Fiske Micro-Osmometer Model 210).

SDS/PAGE

Electrophoresis was performed using standard techniques. Each urine sample was adjusted to an equal creatinine concentration by adding distilled water. The sample was mixed with an equal volume of sample buffer, boiled for 3 min and loaded on to the gel. Protein bands were visualized with Coomassie Brilliant Blue stain (Bio-Rad Laboratories). Albumin band intensities were determined using Scion Image software and quantified by comparison with authentic BSA (Sigma–Aldrich).

Western blot analysis

Western blot analysis was performed with an anti-albumin antibody (R&D Systems) and an HRP (horseradish peroxidase)-conjugated anti-mouse IgG antibody produced in goat (Thermo Scientific Pierce), or with an anti-β_2-microglobulin antibody (Abcam Japan) and an HRP-conjugated anti-rabbit IgG antibody produced in donkey (Thermo Scientific Pierce). Urine samples controlled by creatinine content were applied to a polyacrylamide gel. Following SDS/PAGE (12 % gel), the proteins were transferred electrophoretically on to a Protran® nitrocellulose membrane (Schleicher & Schuell) and visualized with SuperSignal® Chemiluminescent Substrate (Thermo Scientific Pierce).

Light microscopy

Kidneys removed from male 25-week-old G3Stg/GLAko and TgG3S mice were fixed immediately in 10 % Formalin Neutral Buffer Solution (Wako Pure Chemicals) and embedded in paraffin. Paraffin sections (4 μm) were stained with haematoxylin and eosin, and examined by light microscopy.

Gb3 staining with Stx1B (Shiga toxin 1 B) subunit

Frozen tissue sections (10 μm) of 4 % paraformaldehyde-fixed brain and kidneys were incubated with Stx1B (2.5 μg/ml), which binds specifically to Gb3, for 30 min at room temperature, after quenching and blocking of sections. Slides were then incubated with an anti-Stx1B antibody (14 μg/ml) produced in rabbit [18]. Slides were visualized with the Cell & Tissue Staining kit (R&D Systems) according to the manufacturer's protocol. Sections were developed with 3,3'-diaminobenzidine solution for 10 min and counterstained with haematoxylin.

Electron microscopy

Kidneys, brain and aorta were removed from mice and trimmed into small blocks. The blocks were fixed overnight with 2.5 % glutaraldehyde in 0.1 M phosphate buffer (pH 7.4) at 4 °C, and post-fixed for 1 h in 1 % osmium tetroxide in 0.1 M phosphate buffer. Samples were dehydrated in graded ethanol and embedded in Epok-812 (Ohken Shoji). Ultrathin sections (90 nm) were cut on an ultra microtome (Ultracut-N, Reichert Nissei), stained with uranyl acetate and lead citrate, and micrographed with a transmission electron microscope (Hitachi H-600A).

**Table 1   Gb3 content in organs and serum from 20-week-old mice**

Mice ($n > 5$ in each group) were killed at 20 weeks of age, and serum and organs were collected immediately. Gb3 content was determined as described in the Materials and methods section. Values are means $\pm$ S.D. ND, not detectable. The statistical significance of differences in comparison with GLAko mice was determined by Student's t test. *$P < 0.05$; **$P < 0.01$.

(a) Male mice

Organ/serum	Gb3 content (μg/mg of protein in organs; μg/ml in serum)			
	Wild-type	TgG3S	GLAko	G3Stg/GLAko
Heart	ND	0.84 + 0.14	3.20 + 1.20	33.13 + 9.95**
Kidney	0.89 + 0.75	1.81 + 0.87	29.05 + 1.91	57.31 + 8.95**
Spleen	0.09 + 0.07	0.63 + 0.18	14.47 + 0.86	111.95 + 40.33*
Liver	ND	ND	3.04 + 0.56	44.22 + 18.74*
Brain	ND	0.21 + 0.09	0.47 + 0.09	9.02 + 1.48**
Serum	2.25 + 3.00	3.30 + 1.88	6.96 + 1.17	75.52 + 39.32*

(b) Female mice

Organ/serum	Gb3 content (μg/mg of protein in organs; μg/ml in serum)				
	Wild-type	TgG3S	GLAko	G3Stg/GLAko	G3Stg/GLAko ($+/-$)
Heart	ND	2.52 + 0.37	4.92 + 1.02	35.19 + 14.56**	16.22 + 0.77
Kidney	1.00 + 0.44	2.13 + 0.45	24.48 + 6.29	45.92 + 9.53**	29.15 + 4.75
Spleen	0.08 + 0.06	0.72 + 0.10	17.54 + 0.78	74.53 + 8.20**	11.29 + 3.87
Liver	ND	ND	2.57 + 0.86	27.50 + 9.68**	1.08 + 0.79
Brain	ND	0.57 + 0.11	1.22 + 0.14	29.57 + 0.98**	5.24 + 2.41
Serum	3.34 + 1.84	5.18 + 3.75	9.37 + 3.16	23.76 + 1.06**	5.83 + 2.68
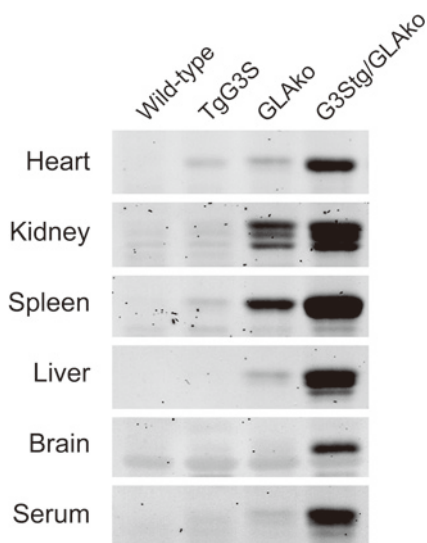
Figure 1   Representative HPTLC results of Gb3 in various mouse strains

Neutral glycolipids extracted from the same volume of serum or an equal protein content of organs of 20-week-old mice were applied to HPTLC plates. Gb3 was separated and stained with orcinol–sulfuric acid.

RESULTS

High Gb3 accumulation in G3Stg/GLAko mouse organs

To determine how overexpressing G3S affects organ Gb3 levels, the neutral glycosphingolipids extracted from major organs of age-matched mice were analysed by HPTLC (high-performance TLC) (Figure 1 and Table 1). The Gb3 levels in the serum and major organs were markedly greater in G3Stg/GLAko mice than in GLAko mice. Compared with wild-type mice, the organ Gb3 content was slightly elevated in TgG3S and markedly higher in G3Stg/GLAko mice. These results indicate that the higher Gb3 accumulations seen in the organs of G3Stg/GLAko mice result from increased Gb3 synthesis and the lack of Gb3 degradation.

Effect of high Gb3 accumulations on the mouse condition and lifespan

Figure 2 shows the body weight and survival of wild-type, TgG3S, GLAko and G3Stg/GLAko mice. Both male and female G3Stg/GLAko mice appeared normal and healthy from birth until 15 weeks of age, after which their body weight gradually decreased (Figure 2A). G3Stg/GLAko mice died by 36 weeks of age, with male and female mice surviving a median 27.6 and 26.7 weeks respectively (Figure 2B). No gross abnormality or early lethality was observed in wild-type, TgG3S or GLAko mice. The G3Stg/GLAko mice began to develop spontaneous tremors, slow movements (Figure 2C), a rounded back (Figure 2D) and gait disturbances at 20 weeks of age. Both male and female G3Stg/GLAko mice tucked their hind limbs to their body when suspended by the tail (Figures 2E and 2G), whereas GLAko and heterozygous G3Stg/GLAko ($+/-$) mice spread their hind limbs (Figures 2F and 2H), as did wild-type and TgG3S mice (results not shown).

Negative association between residual α-Gal A activity and Gb3 accumulation as well as phenotype

We next compared female G3Stg/GLAko mice, which have homozygous *GLA*-null alleles ($-/-$), female G3Stg/GLAko ($+/-$) mice, which have heterozygous *GLA* alleles, and female TgG3S mice, which have normal α-Gal A activity levels. All of these strains expressed the G3S transgene. Figure 3 summarizes the α-Gal A activity and relative Gb3 levels in organs from these three mouse lines; we found that the residual α-Gal A activity negatively correlated with the Gb3 level. The heart and kidney Gb3 levels in the heterozygous G3Stg/GLAko ($+/-$) mice were approximately half those found in the G3Stg/GLAko mice, and the Gb3 levels in the spleen, liver and brain of the heterozygous mice,
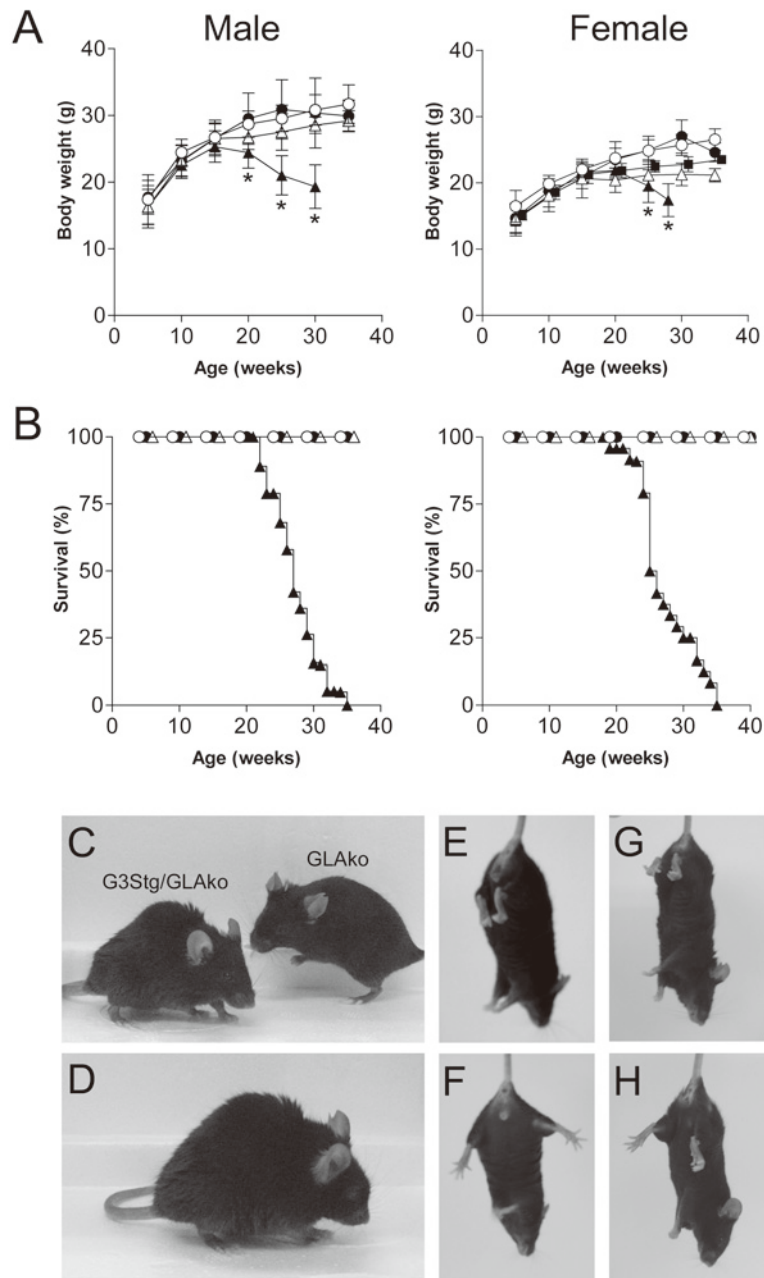
Figure 2   Lifespan and behaviour of G3Stg/GLAko mice

(**A**) Average body weight of male and female wild-type (○), TgG3S (●), GLAko (△), G3Stg/GLAko (▲) and heterozygous G3Stg/GLAko (+ / −) mice (■). The statistical significance of differences in comparison with wild-type mice was determined by Student's t test. *$P < 0.05$. (**B**) Survival curve of male wild-type, TgG3S, GLAko and G3Stg/GLAko mice ($n = 10$, 13, 19 and 24 respectively), and female wild-type, TgG3S, GLAko, G3Stg/GLAko and heterozygous G3Stg/GLAko (+ / −) mice ($n = 16$, 14, 19, 24 and 11 respectively) by the Kaplan–Meier method. Occasional cannibalism and accidental death before 4 weeks of age were not considered. Symbols are the same as in (**A**). (**C**) Representative images of 25-week-old GLAko and G3Stg/GLAko mice and (**D**) a G3Stg/GLAko mouse. (**E–H**) Representative images of posture differences when suspended by the tail. (**E**) A male G3Stg/GLAko mouse, (**F**) a male GLAko mouse, (**G**) a female G3Stg/GLAko mouse and (**H**) a heterozygous G3Stg/GLAko (+ / −) mouse.

which had relatively high α-Gal A activity, were less than 20 % of those in the homozygous mice. The heterozygous G3Stg/GLAko (+ / −) mice appeared healthy, were indistinguishable from female TgG3S mice and had a normal lifespan (Figure 2).

Serum lyso-Gb3 levels

Lyso-Gb3 has been suggested to be useful as a biomarker for diagnosing Fabry disease and for monitoring ERT efficacy [22].

Serum lyso-Gb3 was detectable in GLAko, G3Stg/GLAko and heterozygous G3Stg/GLAko (+ / −) mice, but not in TgG3S or wild-type mice (Table 2).

Gb3 levels in developing mice

We next measured age-related changes in Gb3 accumulation in G3Stg/GLAko and GLAko male mice (Figure 4). Gb3 increased with age in the serum and organs of both G3Stg/GLAko and
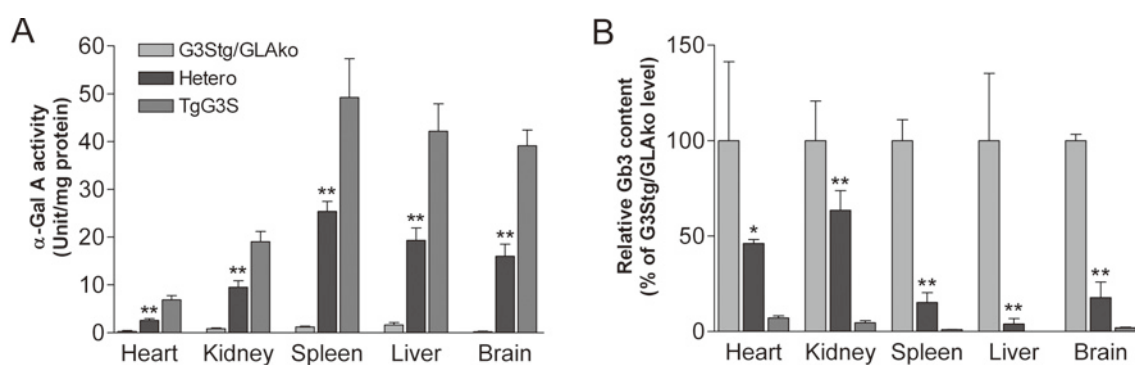
Figure 3   Tissue α-Gal A activity and Gb3 levels in G3S-expressing mouse strains

(**A**) Assays of organ α-Gal A activity in 20-week-old female G3Stg/GLAko, heterozygous G3Stg/GLAko ($+/-$) and TgG3S mice ($n=4$). (**B**) Tissue Gb3 levels relative to the level in female G3Stg/GLAko mice ($n=4$) are shown. Values are means $\pm$ S.D. The statistical significance of differences in comparison with homozygous G3Stg/GLAko mice was determined by Student's t test. $*P < 0.05$; $**P < 0.01$.

Table 2   Serum lyso-Gb3 levels in 20-week-old mice

Serum lyso-Gb3 levels ($n=4$ for each group) were determined as described in the Materials and methods section. Values are means $\pm$ S.D. ND, <10 nM. The statistical significance of differences in comparison with GLAko mice was determined by Student's t test. $**P < 0.01$.

	Serum lyso-Gb3 (nM)				
Gender	Wild-type	TgG3S	GLAko	G3Stg/GLAko	G3Stg/GLAko ($+/-$)
Male	ND	ND	328 ± 25	$518 \pm 72**$	–
Female	ND	ND	302 ± 44	505 ± 209	65 ± 4

GLAko mice, with higher Gb3 levels in the G3Stg/GLAko than in the GLAko mice throughout the experimental period. The heart Gb3 levels measured in G3Stg/GLAko mice at 5, 10, 15, 20 and 25 weeks of age were higher than those in age-matched GLAko mice, by 8.0-, 11.7-, 6.5-, 10.4- and 9.4-fold respectively. Increased Gb3 levels were also seen in the kidney (1.8-, 1.3-, 1.3-, 1.9- and 2.1-fold), spleen (3.9-, 7.0-, 8.5-, 7.7- and 6.8-fold), liver (34.9-, 17.8-, 19.8-, 14.5- and 16.1-fold) and brain (14.9-, 19.3-, 10.7-, 11.5- and 14.2-fold). The serum Gb3 levels were also consistently higher in the G3Stg/GLAko than in the age-matched GLAko mice, with fold increases of 6.4, 7.2, 7.3, 10.1 and 8.6 at 5, 10, 15, 20 and 25 weeks respectively.

Organ weight

GlcCer (glucosylceramide) accumulation causes hepatosplenomegaly in Gaucher disease [23] and its mouse model [24]. Table 3 shows the weight of major organs relative to the body weight in 20-week-old mice. The liver weight in G3Stg/GLAko male mice and spleen weight in G3Stg/GLAko female mice were slightly greater than those in their wild-type counterparts, but were not statistically different from those in GLAko mice. The kidney weight was significantly higher (approximately 1.2-fold) in G3Stg/GLAko mice, both male and female, than in the other three mouse lines. The heart weight was the same in all four lines. No weight change was observed in the organs of heterozygous G3Stg/GLAko ($+/-$) mice compared with those of wild-type mice.
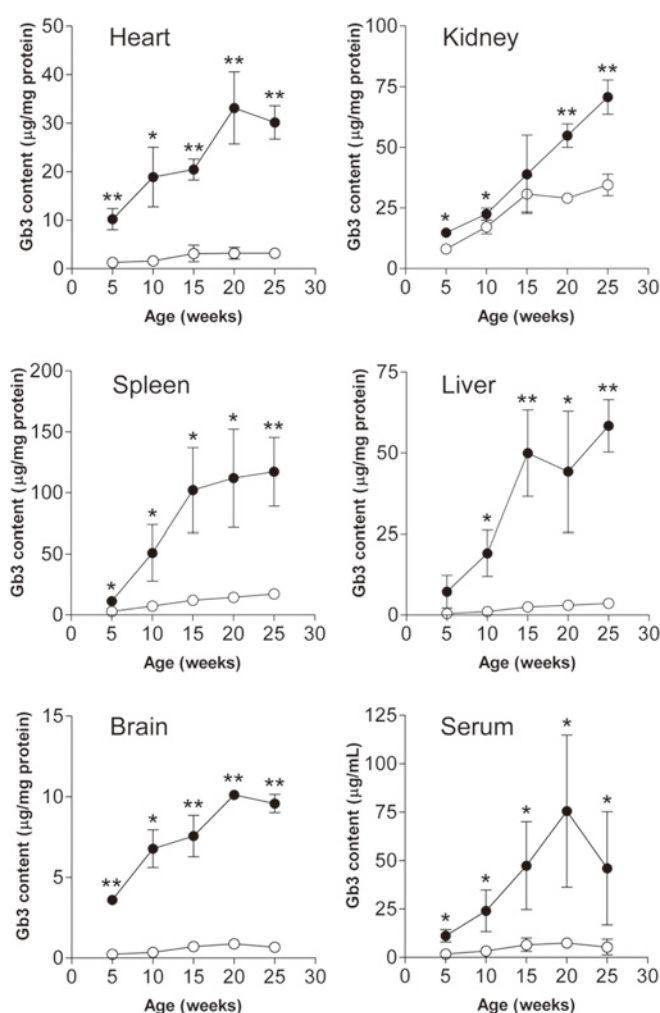

Figure 4   Developmental changes in Gb3 content in the serum and organs of GLAko and G3Stg/GLAko mice

Gb3 content in the serum and organs of male GLAko (○) and G3Stg/GLAko (●) mice at the ages indicated ($n=4$). Values are means $\pm$ S.D. Statistical significance was determined by Student's t test. $*P < 0.05$; $**P < 0.01$.

Table 3   Organ weight of 20-week-old mice

Mice ($n > 5$ for each group) were killed at 20 weeks of age, and organs were immediately collected and weighed. Values are means $\pm$ S.D. The statistical significance of differences in comparison with wild-type mice was determined by Student's t test. *$P < 0.05$; **$P < 0.01$.

(a) Male mice

| Organ | Organ weight in male mice (% of body weight) | | | |
	Wild-type	TgG3S	GLAko	G3Stg/GLAko
Heart	0.375 ± 0.028	0.397 ± 0.018	0.392 ± 0.058	0.390 ± 0.064
Kidney	1.238 ± 0.088	1.277 ± 0.184	1.259 ± 0.108	$1.461 \pm 0.080**$
Spleen	0.252 ± 0.029	0.213 ± 0.032	0.264 ± 0.036	0.278 ± 0.035
Liver	4.286 ± 0.411	4.453 ± 0.548	4.900 ± 0.153	$5.225 \pm 0.394*$

| Organ | Organ weight in female mice (% of body weight) | | | | |
	Wild-type	TgG3S	GLAko	G3Stg/GLAko	G3Stg/GLAko ($+/-$)
Heart	0.449 ± 0.014	0.425 ± 0.043	0.420 ± 0.045	0.421 ± 0.040	0.402 ± 0.026
Kidney	1.192 ± 0.039	1.171 ± 0.175	1.266 ± 0.097	$1.558 \pm 0.450**$	1.242 ± 0.035
Spleen	0.320 ± 0.037	0.296 ± 0.072	0.398 ± 0.092	$0.389 \pm 0.051*$	0.380 ± 0.071
Liver	4.941 ± 0.304	5.081 ± 0.590	5.056 ± 0.549	5.298 ± 0.456	5.468 ± 0.355

Table 4   Effect of ERT on Gb3 content and renal function

G3Stg/GLAko male mice treated with ERT ($n = 5$) were killed at 20 weeks of age, and organs were immediately collected and assayed. Values are means $\pm$ S.D. The statistical significance of differences in comparison with age-matched G3Stg/GLAko male mice was determined by Student's t test. *$P < 0.05$; **$P < 0.01$. ND, not detectable. Values in parenthesis are the percentage of the control.

(a)

Organ	α-Gal A activity (units/mg of protein)	Gb3 content (μg/mg of protein)
Heart	1.7 ± 1.4	$18.31 \pm 1.38**$ (55.3)
Kidney	3.1 ± 1.3	$23.43 \pm 14.43**$ (40.9)
Spleen	$39.6 \pm 12.8**$	$2.38 \pm 1.56**$ (2.1)
Liver	$97.5 \pm 34.7**$	$0.13 \pm 0.23**$ (0.3)
Brain	ND	7.19 ± 3.40 (79.7)

(b)

	α-Gal A activity (units/ml)	Gb3 level (μg/ml)	Lyso-Gb3 level (nM)
Serum	ND	$0.94 \pm 1.27**$ (1.2)	$126 \pm 61**$ (24.3)

(c)

Age	BUN (mg/dl)	Urine volume (ml)	Urinary albumin concentration (mg/mg of creatinine)	Urine osmolality (mOsm/kg)
10-Week-old	–	$1.74 \pm 0.38**$ (68.4)	$0.73 \pm 0.29*$ (61.7)	1479.4 ± 352.5 (112.9)
15-Week-old	–	$2.24 \pm 0.61**$ (60.7)	$0.51 \pm 0.26**$ (53.6)	1310.6 ± 307.6 (119.3)
20-Week-old	50.9 ± 8.1 (79.5)	2.79 ± 0.91 (83.7)	0.43 ± 0.20 (66.3)	945.0 ± 170.6 (100.1)

Renal function

To evaluate how Gb3 accumulation affected renal function, we measured the BUN, urine volume and osmolality (Figure 5), and albuminuria (Figure 6). Compared with age-matched wild-type mice, the BUN levels were not significantly altered in the TgG3S or GLAko mice, but were significantly higher in 20-week-old G3Stg/GLAko mice, both male and female (Figure 5A). BUN was normal in 5-week-old male G3Stg/GLAko mice, but rose progressively and differed significantly from the BUN levels in GLAko mice from 15 weeks of age onwards (Figure 5B).

To determine 24-h urine volume and urine osmolality, mice were housed individually in metabolic cages. In both male and female 20-week-old G3Stg/GLAko mice, the urine volume (approximately 4 ml/day) was significantly higher than that of other lines (approximately 1 ml/day) (Figure 5C). We were unable to determine the urine volume of 5-week-old G3Stg/GLAko mice because they died from stress in the metabolic cages. At 10 weeks of age, the G3Stg/GLAko mice produced a significantly higher volume of urine than GLAko mice, and they produced their highest urine volume at 15 weeks of age (Figure 5D). The average daily water intake of a male 15-week-old G3Stg/GLAko mouse (9 ml/day) was greater than that of an age-matched GLAko mouse (6.4 ml/day). The urine osmolality was significantly lower in the G3Stg/GLAko mice than in the other mice (Figure 5E) from 10 weeks of age onwards (Figure 5F). These data indicate that the kidneys of G3Stg/GLAko mice are less able to concentrate urine. The total urinary creatinine excretion (Figures 5G and 5H) was the same in the G3Stg/GLAko mice and other mouse lines. Although the serum creatinine concentrations were too low to determine
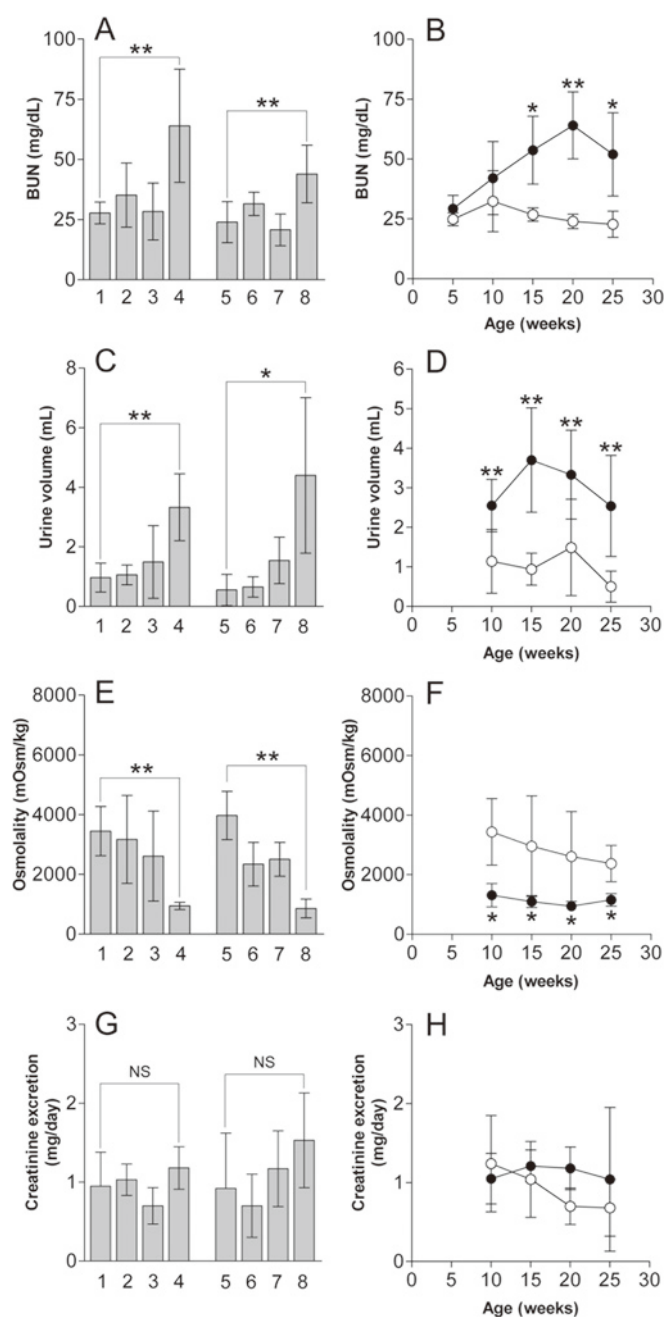
Figure 5   BUN and urine volume of G3Stg/GLAko mice

(**A** and **B**) BUN levels were determined as described in the Materials and methods section. Daily urine volume (**C** and **D**), urine osmolality (**E** and **F**) and urine creatinine excretion (**G** and **H**) were assayed by keeping 20-week-old mice ($n > 4$) in metabolic cages for 24 h (**A, C, E** and **G**). Developmental changes in male GLAko (○) and G3Stg/GLAko (●) mice (**B, D, F** and **H**). (**A**), (**C**), (**E**) and (**G**) Lanes 1 and 5, wild-type mice; lanes 2 and 6, TgG3S mice; lanes 3 and 7, GLAko mice; and lanes 4 and 8, G3Stg/GLAko mice. Lanes 1–4, male mice; and lanes 5–8, female mice. Values are means ± S.D. Statistical significance was determined by Student's t test. $*P < 0.05$; $**P < 0.01$; NS, not significant.

the creatinine clearance precisely, the creatinine clearance may be normal in G3Stg/GLAko mice.

Albuminuria was determined by subjecting mouse urine samples to SDS/PAGE, since a measurable level of low-molecular-mass protein is excreted in mouse urine [25]. High levels of a 67-kDa protein were observed in the urine of both male and female G3Stg/GLAko mice (Figure 6A), and Western blot analysis confirmed that this protein band was albumin (Figure 6B). Since β_2-microglobulin, which is approximately 12-kDa, passes easily through the glomerular basement membrane and is mostly reabsorbed through the proximal tubules, the amount of β_2-microglobulin in the urine provides an index for proximal tubule impairment [26]. Urine from G3Stg/GLAko mice contained detectable amounts of β_2-microglobulin (Figure 6C).

Since low urine osmolality and albuminuria were observed in 10-week-old G3Stg/GLAko mice, we assayed these factors in raw urine samples collected from younger mice. Albuminuria was already present in 3-week-old G3Stg/GLAko mice (Figure 6D). The urinary albumin concentration increased until 9 weeks of age, and decreased slightly thereafter. The highest level of albumin excreted by G3Stg/GLAko mice was 1.28 mg/mg of creatinine, which is still lower than the levels reported in other glomerular-injury mouse models (> 100 mg/mg of creatinine) [27]. Urine osmolality, which was normal in 4-week-old G3Stg/GLAko mice but decreased gradually thereafter, was significantly different from that of GLAko mice from 5 weeks of age onwards (Figure 6E).

Lens

Lens opacities were observed by slit-lamp examination. Moderate 'whitish' granular deposits and diffuse posterior cataract were observed in 7-week-old G3Stg/GLAko mouse eyes (Figure 7). Some deposits were found in the left eye but not in the right eye of a 7-week-old GLAko mouse.

Morphological observation

Although enlarged tubular cells were observed in the G3Stg/GLAko mouse kidneys, there were no structural abnormalities of the Bowman's capsule as are often seen in patients with Fabry disease (Figure 8A). No abnormalities were observed in the kidneys of the other mice, including the TgG3S mice (Figure 8B). An obvious difference between symptomatic G3Stg/GLAko and asymptomatic GLAko mice was observed in the kidney and brain Gb3 immunostaining with Stx1B (Figures 8C–8F). Strong Gb3 staining was seen in the medulla of the kidney and in the cerebral cortex, hippocampus, thalamus and hypothalamus from a 25-week-old G3Stg/GLAko mouse.

Electron microscopy

Electron microscopy revealed large lipid inclusions with electron-dense concentric lamellar structures in the proximal and distal convoluted tubules and collecting ducts from a 25-week-old G3Stg/GLAko mouse (Figures 9A–9C). A small number of lipid inclusions was observed in podocytes, but not in glomelular mesangial cells or endothelial cells (Figure 9D). In brain, lipid inclusions were observed in neurons (Figure 9E) and cells around blood vessels (Figure 9F). We also examined aortic endothelial cells from this mouse, but no lipid inclusion was detected (results not shown).

Effect of ERT on G3Stg/GLAko mice

We next examined whether reducing the Gb3 accumulation by ERT could prevent the renal impairment in the G3Stg/GLAko mice. Male G3Stg/GLAko mice were given injections of recombinant human α-Gal A (1 mg/kg of body weight) at 5, 7, 9, 11, 13, 15, 17 and 19 weeks of age, and were killed at 20 weeks of age. One week after the last injection, the recombinant α-Gal A activity was still high in the spleen and the liver, with
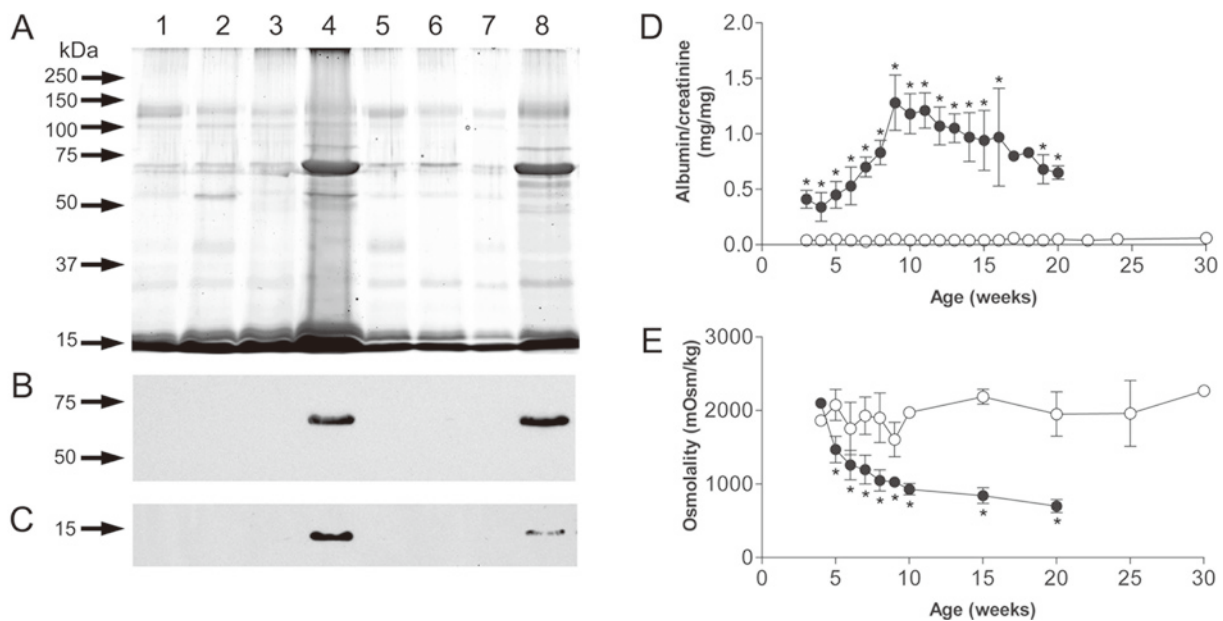
Figure 6   Albuminuria and urine osmolality in G3Stg/GLAko mice

SDS/PAGE analysis (10 % gel) of urine from 15-week-old mice; proteins were stained with Coomassie Brilliant Blue (**A**), and Western blot analysis was performed with an anti-albumin monoclonal antibody (**B**) and an anti-β_2-microglobulin monoclonal antibody (**C**). Lanes 1 and 5, wild-type mice; lanes 2 and 6, TgG3S mice; lanes 3 and 7, GLAko mice; and lanes 4 and 8, G3Stg/GLAko mice. Lanes 1–4, male mice; and lanes 5–8, female mice. The molecular mass in kDa is indicated. (**D** and **E**) Developmental changes in albuminuria (**D**) and urine osmolality (**E**) in male G3Stg/GLAko (●) and GLAko (○) mice were determined from raw urine. Values are means $\pm$ S.D. The statistical significance of the difference in comparison with age-matched GLAko mice was determined by Student's t test. *$P < 0.05$.
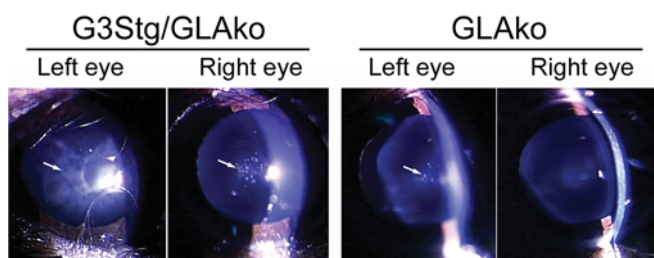

Figure 7   Lenticular opacity

Posterior capsular cataract, visible with slit-lamp microscopy, was observed in male 7-week-old G3Stg/GLAko and GLAko mice. Typical abnormalities are indicated by arrows.

strong clearance of the accumulated Gb3 (Table 4). The clearance of Gb3 in the heart and kidney was relatively small because of the low enzyme distribution to these organs, as described by Ioannou et al. [28]. The serum Gb3 and lyso-Gb3 levels were significantly decreased, and the effect of 1 mg of recombinant α-Gal A/kg on the serum lyso-Gb3 level in the G3Stg/GLAko mice (24.3 % of that in untreated control) corresponded to the effect of ERT on plasma lyso-Gb3 levels in male patients (approximately 25 % of that untreated male patients) [29]. Significant reductions were observed in the urine volume and albumin concentration at 10 and 15 weeks of age, but the urine volume gradually increased. Treatment with 1 mg of recombinant α-Gal A/kg did not change the BUN or urine osmolality. However, in a preliminary experiment with a dose of 3 mg of recombinant α-Gal A/kg, the urine osmolality was much higher in the treated mice (60 % of normal) than in untreated mice (less than 40 % of normal). This indicates that 1 mg of recombinant α-Gal A/kg is not sufficient to block the renal impairment completely

in the G3Stg/GLAko mice. This mouse line may be useful in determining an effective ERT clinical dosage.

DISCUSSION

The results of the present study show that increasing the Gb3 synthesis by overexpressing G3S in the organs promotes phenotypic manifestations in GLAko mice. Both male and female G3Stg/GLAko mice showed early lethality associated with loss of body weight, neurological abnormalities and progressive renal impairment. A decreased ability to concentrate urine, leading to polyuria, is thought to be the first symptom of Fabry disease [4]. The initial symptom in G3Stg/GLAko mice was albuminuria, seen at 3 weeks of age, followed by polyuria at 10 weeks of age. The BUN increased significantly in these mice after 15 weeks of age. In contrast, we saw no abnormalities in GLAko mice during the experimental period. Although there was little difference in the kidney Gb3 level between 5-week-old G3Stg/GLAko and GLAko mice, the serum Gb3 level was 6.4-fold higher in the G3Stg/GLAko than in the GLAko mice. The high Gb3 serum level may increase the accumulation of Gb3 in tubular cells, causing renal impairment in the G3Stg/GLAko mice.

It has been suggested that distal tubular dysfunction, which is most commonly seen in patients with Fabry disease, impairs the kidney's ability to concentrate urine and results in polyuria [4]. The G3Stg/GLAko mice accumulated lamellar inclusion bodies in the proximal and distal convoluted tubules and in collecting ducts. Polyuria and decreased urine osmolality in both the G3Stg/GLAko mice and patients with Fabry disease may result from dysfunctional distal convoluted tubules and collecting ducts. On the other hand, albuminuria might be caused by decreased protein reabsorption at the proximal tubules, since G3Stg/GLAko mice excreted β_2-microglobulin, a sensitive marker for protein
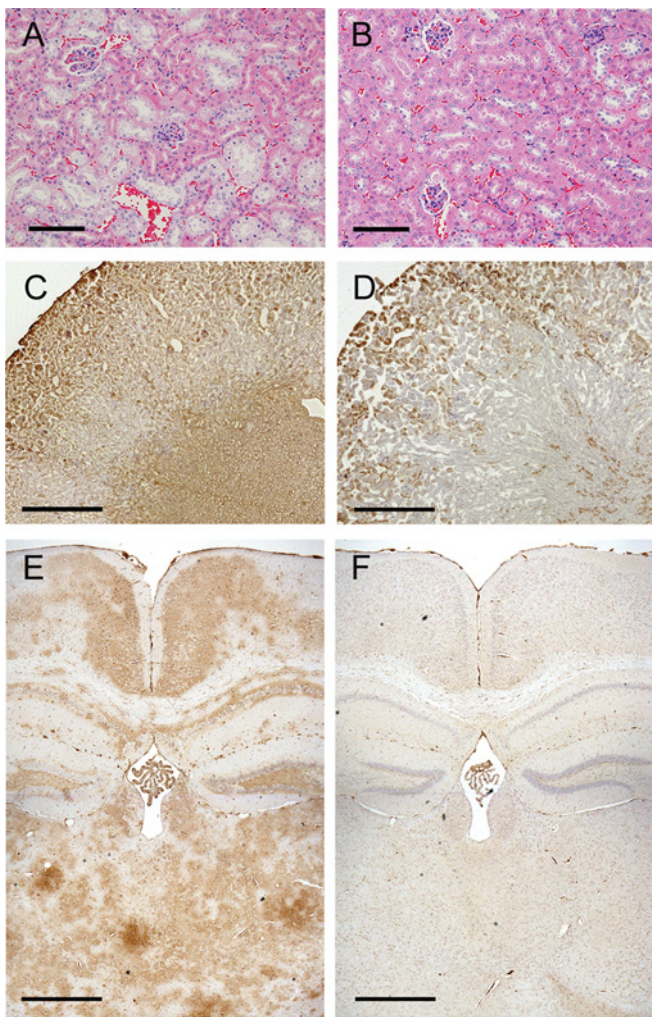
Figure 8   Changes in kidney morphology and Gb3 staining of kidney and brain in G3Stg/GLAko mice

Light microscopy of kidney tissue from 25-week-old male (**A**) G3Stg/GLAko and (**B**) TgG3S mice. Scale bars in (**A**) and (**B**) are 50 μm. The stain is haematoxylin & eosin. Immunohistochemical Gb3 staining with Stx1B in the kidney (**C** and **D**) and the brain (**E** and **F**) from 25-week-old male (**C** and **E**) G3Stg/GLAko and (**D** and **F**) GLAko mice. Scale bars in (**C**–**F**) are 300 μm.

Figure 9   Electron microscopy of the kidney and brain in a 25-week-old G3Stg/GLAko male mouse

(**A**) Proximal tubule, (**B**) distal tubule, (**C**) collecting duct, (**D**) glomerulus (P, podocyte; E, endothelial cell; M, mesangial cell), (**E**) neuronal cell and (**F**) blood vessel in brain. Scale bars are 5 μm. Typical inclusion bodies are indicated by arrows.

reabsorption into the urine through the proximal tubules [26]. G3Stg/GLAko mice between 5 and 20 weeks of age excreted less albumin into the urine than do glomerular-injury model mice [27]. The G3Stg/GLAko mice may have normal glomerular filtration throughout their lifespan, since the level of creatinine excreted into the urine was constant over time and there was no Bowman's capsule abnormality. Patients with Fabry disease often have mild albuminuria and a decreased ability to concentrate urine, even when glomerular filtration rates are normal [30]. These findings indicate that the renal impairment seen in G3Stg/GLAko mice may correspond to the initial steps of renal involvement in patients with Fabry disease. Mild albuminuria at 3 weeks, low urine osmolality at 5 weeks, polyuria at 10 weeks and an increase in BUN at 15 weeks of age should be considered as disease markers for progressive renal impairment in this mouse line.

The plasma lyso-Gb3 levels are markedly abnormal in Fabry patients, especially in females, making it a more sensitive biomarker than plasma Gb3 [31]. In our mouse model, the serum lyso-Gb3 level differed significantly between the heterozygous G3Stg/GLAko $(+/-)$ and female TgG3S mice (65 ± 4 nM
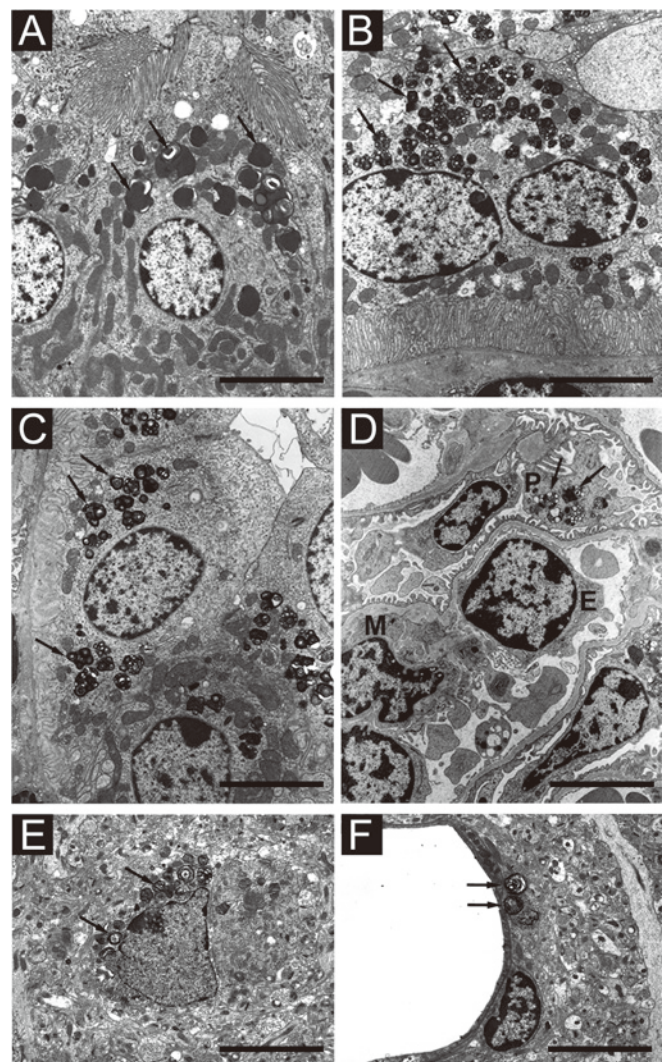
and <10 nM respectively) (Table 2), although their serum Gb3 level was in the same range (5.83 ± 2.68 μg/mg of protein and 5.18 ± 3.75 μg/mg of protein respectively) (Table 1). The differences in serum Gb3 levels between symptomatic G3Stg/GLAko mice and asymptomatic GLAko mice (10.9-fold and 2.5-fold in males and females respectively) were more pronounced than the differences in serum lyso-Gb3 (1.6-fold and 1.7-fold in males and females respectively). These data indicate that although serum lyso-Gb3 is a sensitive marker for deficient α-Gal A activity in mice, it may not correlate well with the symptomatic condition. Urinary albumin excretion and urine osmolality are good symptomatic biomarkers for the renal condition in patients with Fabry disease.

Although hypertrophic cardiomyopathy is a prominent characteristic of Fabry disease, the heart weight was not increased in the G3Stg/GLAko mice. Diastolic and systolic dysfunctions are characteristics of Fabry cardiomyopathy and can usually be detected before the onset of left ventricular hypertrophy [32]. In our preliminary study, G3Stg/GLAko mice (30 weeks

of age) showed reductions in both diastolic and systolic functions compared with wild-type mice by cardiac catheterization. Cardiac failure, renal failure and stroke are the major causes of mortality in Fabry disease [33]. The cause of premature death in G3Stg/GLAko mice is still unknown; at present, we do not have any evidence that their death was associated with heart or kidney defects.

The G3Stg/GLAko mice had neurological abnormalities. Similar phenotypic manifestations have been reported in mouse models for other neuronal disease models, such as GM1-gangliosidosis [34], saposin-B knockout [35] and Huntington's disease [36]. It is very likely that Gb3 accumulation causes neuronal damage that may affect the mortality of the G3Stg/GLAko mice since lamellar inclusions were observed in neuronal cells in this mouse.

All of the symptomatic manifestations in G3Stg/GLAko mice correlated with a loss of α-Gal A activity. We did not observe any symptoms in heterozygous G3Stg/GLAko ($+/-$) mice, which accumulated intermediate amounts of Gb3 in their organs and had approximately half of the α-Gal A activity seen in normal mice. These data indicate that low levels of α-Gal A enzyme activity reduce the symptom severity in G3Stg/GLAko mice. We showed that recombinant α-Gal A treatment at a dosage of 1 mg/kg starting at 5 weeks of age could decrease the urine volume and albumin excretion at 10 and 15 weeks of age. It has been suggested that therapeutic intervention should begin early to protect renal function, since ERT has not been effective in patients with late-stage renal disease [37]. However, the best time to start ERT should be determined based on symptoms, since a strict genotype–phenotype relationship is difficult to define in Fabry disease [38]. G3Stg/GLAko mice should prove useful in experimental ERT studies to determine, for example, the minimum dosage and optimal timing of treatments.

In our present study, we compared G3Stg/GLAko mice and GLAko mice. The mice were often siblings, since G3Stg/GLAko mice carrying the G3S transgene in a single allele were mated with GLAko mice, and the offspring differed only in G3S expression. Thus our mouse data clearly showed that phenotypic manifestations were related to the level of Gb3 produced. Gb3 production can be modified by inflammatory conditions, since inflammatory mediators are known to enhance the Gb3 [39] and G3S expression [40]. G3S expression appears be a critical factor for Gb3 production; this may help to explain the complicated relationship of genotypes to phenotypes in Fabry disease.

One option for treating lysosomal storage diseases is SRT [41]. NB-DNJ (N-butyldeoxynojirimycin) is the only SRT approved for Gaucher's disease type 1 [42]. NB-DNJ potently inhibits GlcCer synthase, which is the first step in glycosphingolipid synthesis. Our present data indicate that Gb3 synthase may be another SRT target in Fabry disease. Inhibiting the Gb3 production in G3Stg/GLAko mice may diminish or slow the onset of phenotypic manifestations, since GLAko mice with low Gb3 expression are asymptomatic. Thus the G3Stg/GLAko mouse will be a useful experimental model for preclinical studies of SRT drug candidates.

Although GLAko mice lack a spontaneous vascular phenotype, they have been used as experimental models of thrombosis [43] and atherosclerosis [44]. In our preliminary determination, Gb3 content in aorta from G3Stg/GLAko mice was 4-fold higher than that from GLAko mice. G3Stg/GLAko mice will also be useful for studying the pathogenesis of vascular manifestations, because abnormalities of the aortic endothelial cells are observed depending on the Gb3 accumulation [45].

In conclusion, we have generated a mouse model that mimics Fabry disease with renal impairment, and this progressive renal impairment was achieved by increasing Gb3 accumulation in a GLA-null background. This is the first clear evidence that significant Gb3 accumulation is the primary cause of Fabry disease. Our G3Stg/GLAko mouse model will be useful for studying the pathogenesis of Fabry disease and for preclinical studies of drug candidates.

AUTHOR CONTRIBUTION

Atsumi Taguchi, Hiroki Maruyama, Hidekatsu Yoshioka and Satoshi Ishii conceived and designed experiments, and wrote the paper. Atsumi Taguchi and Satoshi Ishii performed all of the experiments, except for Figure 9, which was undertaken by Hiroki Maruyama, Masaaki Nameta and Tadashi Yamamoto. Junichiro Matsuda and Ashok Kulkarni provided transgenic mouse lines and insightful advice for animal experiments. All of the authors were involved in the critical review of the paper prior to submission.

ACKNOWLEDGEMENTS

FUNDING

REFERENCES

1 Brady, O. R., Gal, A. E., Bradley, R. M., Martensson, E., Warshaw, A. L. and Laster, L. (1967) Enzymatic defect in Fabry's disease: ceramidetrihexosidase deficiency. N. Engl. J. Med. **276**, 1163–1167

2 Desnick, R. J., Ioannou, Y. A. and Eng, C. M. (2001) α-Galactosidase A deficiency: Fabry disease. In The Metabolic and Molecular Bases of Inherited Disease (Scriver, C. R., Beaudet, A. L., Sly, W. S. and Valle, D., eds), pp. 3733–3774, McGraw-Hill, New York

3 Shah, J. S. and Elliott, P. M. (2005) Fabry disease and the heart: an overview of the natural history and the effect of enzyme replacement therapy. Acta Paediatr. Suppl. **94**, 11–14

4 Branton, M., Schiffmann, R. and Kopp, J. B. (2002) Natural history and treatment of renal involvement in Fabry disease. J. Am. Soc. Nephrol. **13** (Suppl. 2), S139–S143

5 Wilcox, W. R., Oliveira, J. P., Hopkin, R. J., Ortiz, A., Banikazemi, M., Feldt-Rasmussen, U., Sims, K., Waldek, S., Pastores, G. M., Lee, P. et al. (2008) Females with Fabry disease frequently have major organ involvement: lessons from the Fabry Registry. Mol. Genet. Metab. **93**, 112–128

6 Ohshima, T., Murray, G. J., Swaim, W. D., Longenecker, G., Quirk, J. M., Cardarelli, C. O., Sugimoto, Y., Pastan, I., Gottesman, M. M., Brady, R. O. and Kulkarni, A. B. (1997) α-Galactosidase A deficient mice: a model of Fabry disease. Proc. Natl. Acad. Sci. U.S.A. **94**, 2540–2544

7 Ohshima, T., Schiffmann, R., Murray, G. J., Kopp, J., Quirk, J. M., Stahl, S., Chan, C. C., Zerfas, P., Tao-Cheng, J. H., Ward, J. M. et al. (1999) Aging accentuates and bone marrow transplantation ameliorates metabolic defects in Fabry disease mice. Proc. Natl. Acad. Sci. U.S.A. **96**, 6423–6427

8 Schiffmann, R. S., Kopp, J. B., Austin, H. A., Sabnis, S., Moore, D. F., Wiebel, T., Balow, J. E. and Brady, R. O. (2001) Enzyme replacement therapy in Fabry disease. JAMA, J. Am. Med. Assoc. **285**, 2743–2749

9 Eng, C. M., Guffon, N., Wilcox, W. R., Germain, D. P., Lee, P., Waldek, S., Caplan, L., Linthorst, G. E., Desnick, R. J. and International Collaborative Fabry Disease Study Group (2001) Safety and efficacy of recombinant human α-galactosidase A replacement therapy in Fabry's disease. N. Engl. J. Med. **345**, 9–16

10 Beutler, E. (2006) Lysosomal storage diseases: natural history and ethical and economic aspects. Mol. Genet. Metab. **88**, 208–215

11 Linthorst, G. E., Hollak, C. E., Donker-Koopman, W. E., Strijland, A. and Aerts, J. M. (2004) Enzyme therapy for Fabry disease: neutralizing antibodies toward agalsidase α and β. Kidney Int. **66**, 1589–1595

12 Takenaka, T., Murray, G. J., Qin, G., Quirk, J. M., Ohshima, T., Qasba, P., Clark, K., Kurkarni, A. B., Brady, R. O. and Medin, J. A. (2000) Long-term enzyme correction and lipid reduction in multiple organs of primary and secondary transplanted Fabry mice receiving transduced bone marrow cells. Proc. Natl. Acad. Sci. U.S.A. **97**, 7515–7520

13 Abe, A., Gregoory, S., Lee, L., Killen, P. D., Brady, R. O., Kulkarni, A. B. and Shayman, J. A. (2000) Reduction of globotriaosylceramide in Fabry disease mice by substrate deprivation. J. Clin. Invest. **105**, 1563–1571

14 Marshall, J., Ashe, K. M., Bangari, D., McEachern, K., Chuang, W. L., Pacheco, J., Copeland, D. P., Desnick, R. J., Shayman, J. A., Scheule, R. K. and Cheng, S. H. (2010) Substrate reduction augments the efficacy of enzyme therapy in a mouse model of Fabry disease. PLoS ONE **5**, e15033

15 Fan, J.-Q., Ishii, S., Asano, N. and Suzuki, Y. (1999) Accelerated transport and maturation of lysosomal a-galactosidase A in Fabry lymphoblasts by an enzyme inhibitor. Nat. Med. **5**, 112–115

16 Ishii, S. (2012) Pharmacological chaperone therapy for Fabry disease. Proc. Jpn. Acad., Ser. B **88**, 18–30

17 Ashe, K. M., Bangari, D., Li, L., Cabrera-Salazar, M. A., Bercury, S. D., Nietupski, J. B., Cooper, C. G., Aerts, J. M., Lee, E. R., Copeland, D. P. et al. (2011) Iminosugar-based inhibitors of glucosylceramide synthase increase brain glycosphingolipids and survival in a mouse model of Sandhoff disease. PLoS ONE **6**, e21758

18 Shiozuka, C., Taguchi, A., Matsuda, J., Noguchi, Y., Kunieda, T., Uchio-Yamada, K., Yoshioka, H., Hamanaka, R., Yano, S., Yokoyama, S. et al. (2011) Increased globotriaosylceramide levels in a transgenic mouse expressing human α1,4-galactosyltransferase and a mouse model for treating Fabry disease. J. Biochem. **149**, 161–170

19 Ishii, S., Yoshioka, H., Mannen, K., Kulkarni, A. B. and Fan, J.-Q. (2004) Transgenic mouse expressing human mutant α-galactosidase A in an endogenous enzyme deficient background: a biochemical animal model for studying active-site specific chaperone therapy for Fabry disease. Biochim. Biophys. Acta **1690**, 250–257

20 Ishii, S., Chang, H.-H., Yoshioka, H., Shimada, T., Mannen, K., Higuchi, Y., Taguchi, A. and Fan, J.-Q. (2009) Preclinical efficacy and safety of 1-deoxygalactonojirimycin in mice for Fabry disease. J. Pharmacol. Exp. Ther. **328**, 723–731

21 Maruyama, H., Takata, T., Tsubata, Y., Tazawa, R., Goto, K., Tohyama, J., Narita, I., Yoshioka, H. and Ishii, S. (2013) Screening of male dialysis patients for Fabry disease by plasma globotriaosylsphingosine. Clin. J. Am. Soc. Nephrol. **8**, 629–636

22 Aerts, J. M., Groener, J. E., Kuiper, S., Donker-Koopman, W. E., Strijland, A., Ottenhoff, R., van Roomen, C., Mirzaian, M., Wijburg, F. A., Linthorst, G. E. et al. (2008) Elevated globotriaosylsphingosine is a hallmark of Fabry disease. Proc. Natl. Acad. Sci. U.S.A. **105**, 2812–2817

23 Beutler, E. and Grabowski, G. A. (2001) Gaucher disease. In The Metabolic and Molecular Bases of Inherited Disease (Scriver, C. R., Beaudet, A. L., Sly, W. S. and Valle, D., eds), pp. 3635–3668, McGraw-Hill, New York

24 Enquist, I. B., Nilsson, E., Ooka, A., Månsson, J. E., Olsson, K., Ehinger, M., Brady, R. O., Richter, J. and Karlsson, S. (2006) Effective cell and gene therapy in a murine model of Gaucher disease. Proc. Natl. Acad. Sci. U.S.A. **103**, 13819–13824

25 Leheste, J. R., Rolinski, B., Vorum, H., Hilpert, J., Nykjaer, A., Jacobsen, C., Aucouturier, P., Moskaug, J. O., Otto, A., Christensen, E. I. and Willnow, T. E. (1999) Megalin knockout mice as an animal model of low molecular weight proteinuria. Am. J. Pathol. **155**, 1361–1370

26 Gerritsen, K. G., Peters, H. P., Nguyen, T. Q., Koeners, M. P., Wetzels, J. F., Joles, J. A., Christensen, E. I., Verroust, P. J., Li, D., Oliver, N. et al. (2010) Renal proximal tubular dysfunction is a major determinant of urinary connective tissue growth factor excretion. Am. J. Physiol. Renal Physiol. **298**, F1457–F1464

27 Heymann, F., Meyer-Schwesinger, C., Hamilton-Williams, E. E., Hammerich, L., Panzer, U., Kaden, S., Quaggin, S. E., Floege, J., Gröne, H. J. and Kurts, C. (2009) Kidney dendritic cell activation is required for progression of renal disease in a mouse model of glomerular injury. J. Clin. Invest. **119**, 1286–1297

28 Ioannou, Y. A., Zeidner, K. M., Gordon, R. E. and Desnick, R. J. (2001) Fabry disease: preclinical studies demonstrate the effectiveness of α-galactosidase A replacement in enzyme-deficient mice. Am. J. Hum. Genet. **68**, 14–25

29 Boutin, M., Gagnon, R., Lavoie, P. and Auray-Blais, C. (2012) LC-MS/MS analysis of plasma lyso-Gb3 in Fabry disease. Clin. Chim. Acta **414**, 273–280

30 Tondel, C., Bostad, L., Hirth, A. and Svarstad, E. (2008) Renal biopsy findings in children and adolescents with Fabry disease and minimal albuminuria. Am. J. Kidney Dis. **51**, 767–776

31 Rombach, S. M., Dekker, N., Bouwman, M. G., Linthorst, G. E., Zwinderman, A. H., Wijburg, F. A., Kuiper, S., Vd Bergh Weerman, M. A., Groener, J. E., Poorthuis, B. J. et al. (2010) Plasma globotriaosylsphingosine: diagnostic value and relation to clinical manifestations of Fabry disease. Biochim. Biophys. Acta **1802**, 741–748

32 Pieroni, M., Chimenti, C., Ricci, R., Sale, P., Russo, M. A. and Frustaci, A. (2003) Early detection of Fabry cardiomyopathy by tissue Doppler imaging. Circulation **107**, 1978–1984

33 Mehta, A., Ricci, R., Widmer, U., Dehout, F., Garcia de Lorenzo, A., Kampmann, C., Linhart, A., Sunder-Plassmann, G., Ries, M. and Beck, M. (2004) Fabry disease defined: baseline clinical manifestations of 366 patients in the Fabry Outcome Survey. Eur. J. Clin. Invest. **34**, 236–242

34 Matsuda, J., Suzuki, O., Oshima, A., Ogura, A., Naiki, M. and Suzuki, Y. (1997) Neurological manifestations of knockout mice with β-galactosidase deficiency. Brain Dev. **19**, 19–20

35 Sun, Y., Witte, D. P., Ran, H., Zamzow, M., Barnes, S., Cheng, H., Han, X., Williams, M. T., Skelton, M. R., Vorhees, C. V. and Grabowski, G. A. (2008) Neurological deficits and glycosphingolipid accumulation in saposin B deficient mice. Hum. Mol. Genet. **17**, 2345–2356

36 Sadagurski, M., Cheng, Z., Rozzo, A., Palazzolo, I., Kelley, G. R., Dong, X., Krainc, D. and White, M. F. (2011) IRS2 increases mitochondrial dysfunction and oxidative stress in a mouse model of Huntington disease. J. Clin. Invest. **121**, 4070–4081

37 Schiffmann, R., Ries, M., Timmons, M., Flaherty, J. T. and Brady, R. O. (2006) Long-term therapy with agalsidase α for Fabry disease: safety and effects on renal function in a home infusion setting. Nephrol., Dial., Transplant. **21**, 345–354

38 Ries, M. and Gal, A. (2006) Genotype-phenotype correlation in Fabry disease. In Fabry Disease: Perspectives from 5 years of FOS (Mehta, A., Beck, M. and Sunder-Plassmann, G., eds), pp. 331–336, Oxford PharmaGenesis, Oxford

39 Eisenhauer, P. B., Chaturvedi, P., Fine, R. E., Ritchie, A. J., Pober, J. S., Cleary, T. G. and Newburg, D. S. (2001) Tumor necrosis factor α increases human cerebral endothelial cell Gb3 and sensitivity to Shiga toxin. Infect. Immun. **69**, 1889–1894

40 Stricklett, P. K., Hughes, A. K., Ergonul, Z. and Kohan, D. E. (2002) Molecular basis for up-regulation by inflammatory cytokines of Shiga toxin 1 cytotoxicity and globotriaosylceramide expression. J. Infect. Dis. **186**, 976–982

41 Radin, N. S. (1996) Treatment of Gaucher's disease with an enzyme inhibitor. Glycoconjugate J. **13**, 153–157

42 Cox, T., Lachmann, R., Hollak, C., Aerts, J., van Weely, S., Hrebicek, M., Platt, F., Butters, T., Dwek, R., Moyses, C. et al. (2000) Novel oral treatment of Gaucher's disease with N-butyldeoxynojirimycin (OGT 918) to decrease substrate biosynthesis. Lancet **355**, 1481–1485

43 Eitzman, D. T., Bodary, P. F., Shen, Y., Khairallah, C. G., Wild, S. R., Abe, A., Shaffer-Hartman, J. and Shayman, J. A. (2003) Fabry disease in mice is associated with age-dependent susceptibility to vascular thrombosis. J. Am. Soc. Nephrol. **14**, 298–302

44 Bodary, P. F., Shen, Y., Vargas, F. B., Bi, X., Ostenso, K. A., Gu, S., Shayman, J. A. and Eitzman, D. T. (2005) α-Galactosidase A deficiency accelerates atherosclerosis in mice with apolipoprotein E deficiency. Circulation **111**, 629–632

45 Shu, L., Murphy, H. S., Cooling, L. and Shayman, J. A. (2005) An *in vitro* model of Fabry disease. J. Am. Soc. Nephrol. **16**, 2636–2645